IEEE Access
Multidisciplinary | Rapid Review | Open Access Journal

Received June 17, 2020, accepted July 15, 2020, date of publication July 29, 2020, date of current version August 10, 2020.

Digital Object Identifier 10.1109/ACCESS.2020.3012787

An All-Metal High-Gain Radial-Line Slot-Array Antenna for Low-Cost Satellite Communication Systems

MST NISHAT YASMIN KOLI[1], (Graduate Student Member, IEEE), MUHAMMAD U. AFZAL[2], (Member, IEEE), KARU P. ESSELLE[2], (Fellow, IEEE), AND RAHEEL M. HASHMI[1], (Member, IEEE)

[1]School of Engineering, Macquarie University, Sydney, NSW 2109, Australia
[2]School of Electrical and Data Engineering, University of Technology Sydney, Sydney, NSW 2007, Australia

Corresponding author: Mst Nishat Yasmin Koli (mst-nishat-yasmin.koli@students.mq.edu.au)

This work was supported in part by the International Macquarie University Research Excellence Scholarship (iMQRES) Scheme, and in part by the Australian Research Council Discovery grant.

ABSTRACT This article presents a method to produce a highly directive circularly polarized radiation beam (gain>35 dBi) from an all-metal circularly polarized radial-line slot array (RLSA) antenna. The antenna comprises a single-layer radial TEM waveguide, fully filled with air, formed between a metal ground plate and a parallel metal slotted sheet, leading to simple, low-cost fabrication. A prototype of the new antenna having a diameter of 0.4 m or $27\lambda_0$, where λ_0 is the free-space wavelength at the operating frequency of 20 GHz, was fabricated and tested. Its measured peak broadside directivity and measured peak realized gain are 36.3 dBic and 35.9 dBic, respectively. The total thickness of the antenna is only 6.5 mm or $0.43\lambda_0$. The aperture efficiency of the prototype is 56%, total efficiency is 95.4%, and measured 3-dB axial ratio bandwidth is 4.9 GHz (22.9%). The antenna has excellent cross-polar rejection, with a measured cross-polar level of −24.4 dB in the broadside direction. This antenna has been targeted for low-cost SATCOM terminals and wireless backhauls but due to the lack of dielectrics, it may also be useful for space and high-power microwave applications.

INDEX TERMS Circularly polarized, CP, RLSA, metal, low cost, high gain, pattern quality, LHCP, RHCP, slot array, SATCOM, WTM, SOTM, COTM, 5G, 6G, slot array.

I. INTRODUCTION

As a result of existing and upcoming data-hungry devices and services, there is a growing interest among satellite operators to provide broadband internet connectivity to moving platforms anywhere anytime, such as airplanes, trains, emergency and rescue vehicles, defense vehicles and long-distance buses. A vital component of a mobile satellite communication terminal, also known as satellite-on-the-move (SOTM), is a low-profile high-gain antenna with beam steering capability [1]. A recently invented Near-Field Meta-Steering method [1] requires a low-profile, high-gain antenna with a fixed beam as the base antenna. In order to cater to a wide range of mass markets, the antenna design should be amenable to low-cost manufacturing in large quantities.

The associate editor coordinating the review of this manuscript and approving it for publication was Nagendra Prasad Pathak.

Radial line slot array (RLSA) antennas introduced by Kelly in early 1960s [2] are known for their highly directive radiation characteristics. This naturally low-profile antenna concept was later extended by Ando and Goto in the 1980s [3]–[9]. An RLSA comprises a radial thin TEM waveguide formed between two parallel metal plates and can be designed to radiate either linear or circular polarization. Linearly polarized RLSAs have slots arranged in concentric circles, whereas circularly polarized (CP) RLSAs have slots arranged in a spiral [10]–[18]. The top plate has radiating slots while the bottom plate is the ground plane. At the centre of the cavity, there is a feeding probe to excite an outward travelling TEM wave.

In a typical RLSA antenna, the radiating slots forming the top plate are printed on a low-loss commercially available dielectric laminate [10], [19]–[28]. The use of low-loss commercial dielectric laminates, particularly for

a SATCOM antenna that can have lateral dimensions as large as twenty-five free-space wavelengths, increases the antenna material cost and make them unattractive for low-cost systems.

The aim of this research is to develop a low-cost circularly polarized RLSA antenna with a fixed broadside beam. Conventional CP RLSAs used a dielectric layer or a slow-wave structure to avoid grating lobes. We present here a CP-RLSA antenna that is made with all-metal and does not require dielectrics or any other slow-wave structure, significantly reducing the manufacturing complexity, cost and weight of the antenna. The typical design principle in previous CP-RLSAs is to allow one guided wavelength gap between unit radiators along the radial direction at the centre frequency [3], [4], [10]. The rationale to insert a dielectric layer or other wave-slowing devices to the waveguide is that without them the guided-wavelength within the waveguide (λ_g) is equal to the free space wavelength (λ_0) and one λ_0 gap between unit radiators produces grating lobes. In the proposed RLSA we choose a radically different design principle to make the antenna all-metal, that means the waveguide is totally air-filled with no dielectric whatsoever, and the unit radiators are arrayed along the radial and spiral directions by a certain distance. This prevents the onset of grating lobes within the operating frequency range without having to insert dielectrics or other wave-slowing structures, significantly reducing the manufacturing complexity, cost and weight of the antenna.

In contrast to previously reported printed RLSAs, the proposed design can be mass-produced using standard sheets of metal. As this design does not require dielectrics, a phase tuning structure, a mode converter, reflection cancelling slots or absorbers its configuration is much simpler than the double-layered dielectric-less RLSAs [26], [29], [30]. In this design, RF losses are extremely low, which greatly enhance the total antenna efficiency. Since there is no dielectric material in the waveguide, the antenna can also be used for high power microwave applications and in space where dielectric ionization can be problematic.

The article is arranged such that the antenna design methodology and related theory are given in Section II. Section III describes how antenna parameters affect their performance. Predicted and measured results are presented in Section IV.

II. DESIGN

A perspective view of the new antenna is shown in Fig. 1. The two parallel metal plates form a radial waveguide, which is filled with air. The upper plate has radiating slots. The lower plate is the ground plane. The radial waveguide is excited at the centre by an SMA connector. The top end of the connector has a disk-ended feed probe which generates a radially outward travelling TEM wave in the waveguide.

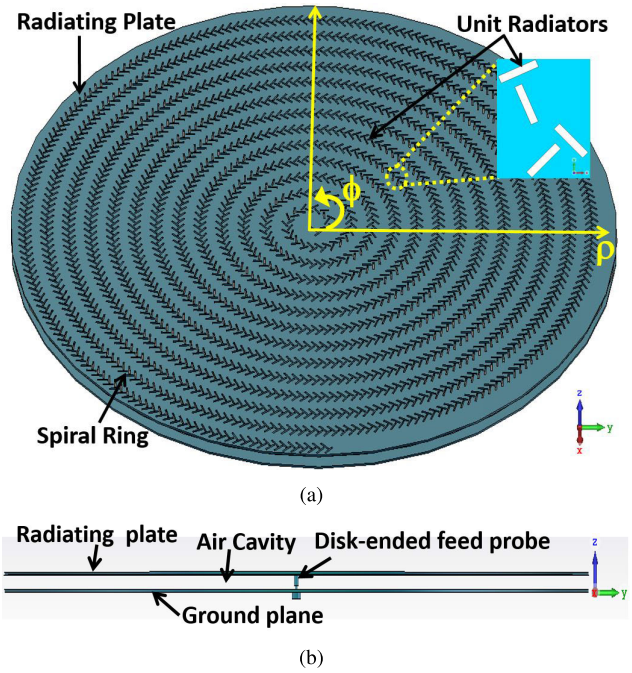

FIGURE 1. Configuration of the new all-metal CP-RLSA antenna (a) A perspective view of the RLSA, (b) Cross-section of the RLSA.

A. WAVEGUIDE CAVITY OPERATION AND FEED STRUCTURE

To explain the mechanism of the radial waveguide, a close-up view of it, with the radiating slots on the top surface, is shown in Fig. 2. The waveguide is filled with air and supports a symmetrical transverse electromagnetic wave mode. A modified dielectric-coated 50Ω SMA connector is inserted from the ground plane to feed the waveguide. The connector end has a disk-head, which converts the power from the outward travelling transverse electromagnetic (TEM) coaxial mode into the TEM waveguide mode. The disk-head is made of aluminium and entirely resides inside the air-filled waveguide. The slots

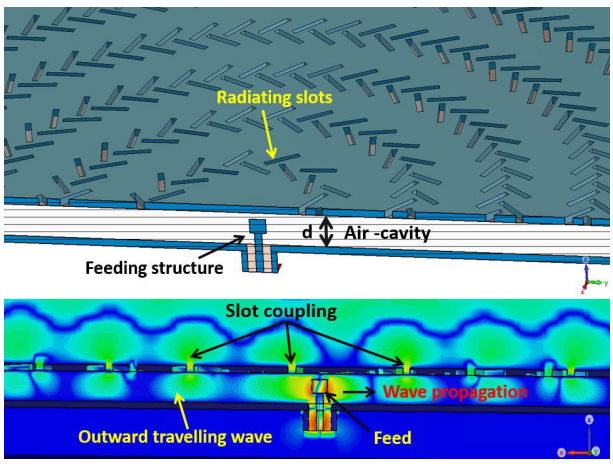

FIGURE 2. Wave propagation inside the waveguide cavity.

on the top plate intercept the radial currents travelling outwardly within the waveguide. As the height of the waveguide (d) is less than half of the wavelength ($d < \lambda_0/2$) where λ_0 is the free-space wavelength at the operating frequency, then the only possible symmetrical mode travelling within the cavity is the TEM mode whose magnetic field is given by [3]:

$$H_\phi(\rho) = H_1^{(2)}(k\rho) - \tau \frac{H_1^{(2)}(k\rho_{max})}{H_1^{(1)}(k\rho_{max})} H_1^{(1)}(k\rho) \quad (1)$$

where ρ = Radial position
$H_1^{(1)}(k\rho)$ = Hankel function of the first kind of order one
$H_1^{(2)}(k\rho)$ = Hankel function of the second kind of order one
$k = 2\pi/\lambda_o$ is the wave number in the radial waveguide
τ = Reflection coefficient at the end of the radial waveguide

In equation (1), the first term represents the outward travelling wave produced by the SMA connector and the second term represents the inward travelling waves created due to the reflections at the end of the TEM waveguide. For a large aperture, the power reaching the end is considerably small, so the waveguide end can be left open. Also, the inward travelling waves (second term) only contribute to cross-polarization and have no impact on co-polar radiation. Therefore, for large antennas, the reflection coefficient is presumed to be negligible ($\tau \to 0$) and the second term in equation (1) can be neglected to give:

$$H_\phi(\rho) \approx H_1^{(2)}(k\rho) \quad (2)$$

If $k\rho \gg 1$, we can simplify the equation as

$$H_\phi(\rho) \approx \sqrt{\frac{2}{\pi k\rho}} e^{-j(k\rho - 3\pi/4)} \quad (3)$$

Slot excitation (equivalent magnetic current) F is proportional to the field inside the waveguide, and its variation with radial distance can be approximated by [10]

$$F(\rho) \propto e^{-jk\rho} \quad (4)$$

where k_ρ is the wave number in the radial waveguide. Since the waveguide magnetic field has only ϕ-component, the only existing surface current is the radial current, proportional to H_ϕ. For a given slot, the field coupled to that slot is proportional to the inner field and to the sine of the slot orientation angle.

$$F = e^{-jk\rho} \cdot sin\theta_1 \quad (5)$$

where θ_1 represents the angle of the respective slot makes with the current flow line as shown in Fig. 4.

In this antenna design, the height (d) of the waveguide is selected to be 5 mm, which is less than half of the free space wavelength ($\lambda_0/2 \approx 7.5$ mm). Therefore, only TEM mode propagates through the waveguide. To ensure optimal power transfer, a feed structure was designed and optimised through parametric analysis in CST Microwave Studio. Fig. 3 shows the configuration of the feed structure. The main requirement of the feed design was to achieve a return loss greater than or equal to 10 dB. The coaxial pin was made with copper, and the coaxial line was filled with Teflon (PTFE-lossy; epsilon 2.1). Table 1 summarises the feed structure design parameter.

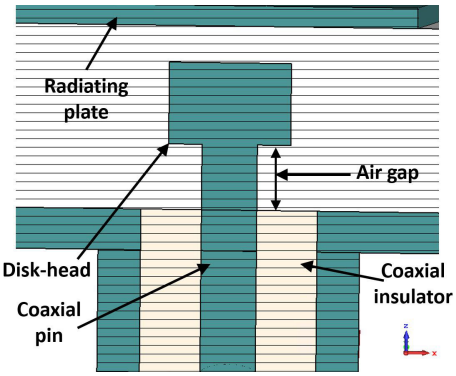

FIGURE 3. Configuration of the feed.

TABLE 1. Feed structure design parameter.

Parameter	Value (mm)
Thickness of the disk-head	2
Radius of the disk-head	1.4
Air gap below disk-head	1.6
Radius of the coaxial pin	0.65
Width of the coaxial insulator	1.4

B. A UNIT RADIATOR DESIGN

The next step is to design the fundamental radiating unit consisting of two orthogonal slots. One such unit radiator, at a hypothetical location on the aperture, is shown in Fig. 4. The two slots (Slot1 and Slot2) of the unit radiator are spatially orthogonal. The distance from the origin O (centre of the antenna aperture) to the centre of Slot1 and Slot2 is ρ_1 and ρ_2, respectively. The point O on RLSA radiating plate is also the location of the feed probe and the point of origin of the outward travelling TEM wave. A straight line from O to the centre of slot indicates the ideal current-flow line. The two slots in the slot pair are oriented such that they make an angle of θ_1 and θ_2 with their respective current flow lines. The length and width of each slot are represented by L and W, respectively, which are same for the two slots in a unit radiator but may be different for slots in different unit radiators. θ_1 is 45° and θ_2 is $45° + \theta$.

It is well known that circular polarization can be achieved when the magnitudes of two spatially orthogonal field components are identical, but their phases differ by an odd multiple of $\pi/2$. Since the two slots in the pair are spatially orthogonal, they generate two orthogonal field components. Furthermore, the two slots in the pair are physically separated such that the electric fields radiated by the two slots have a phase difference of $\pi/2$. The Slot1 and Slot2 produce electric field vectors E_1 and E_2, respectively.

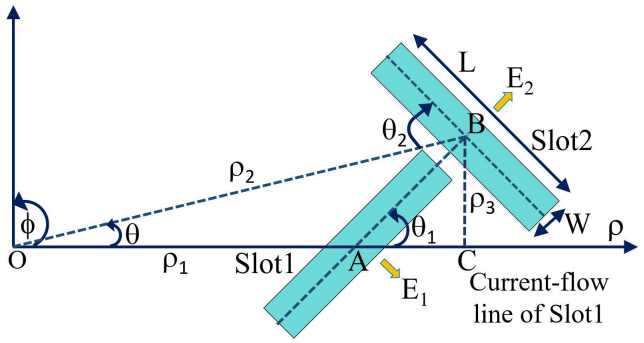

FIGURE 4. Orthogonal slot pair that acts as the unit radiator of a CP-RLSA antenna.

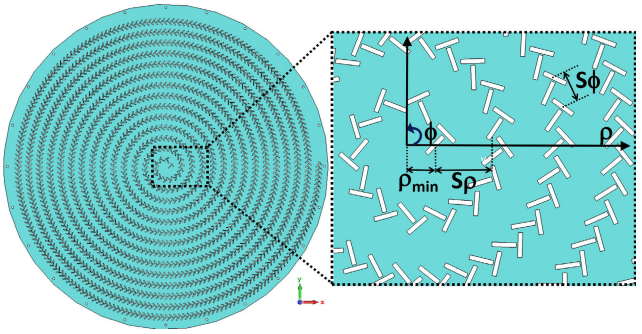

FIGURE 5. Arranging the unit radiators on the top surface of the RLSA.

The actual phase difference between the two slots in the unit radiator depends on ρ_2 - ρ_1, which is the path difference in current-flow lines of the two slots. The phase difference between the two orthogonal slots ($\Delta\phi$) is given by

$$\Delta\phi = \frac{2\pi(\rho_2 - \rho_1)}{\lambda_g} \tag{6}$$

where λ_g is the guided wavelength of the TEM wave. To obtain right-hand circular polarization the phase difference must be equal to $\pi/2 + n\pi$ (where n = 0, 1, 2 . . .). For n = 0, this leads to

$$\rho_2 - \rho_1 = \frac{\lambda_g}{4} \tag{7}$$

Thus the minimum path difference between the two orthogonal slots must be one-fourth of the guided wavelength. To excite both slots with the same magnitude let us make $\theta_1 = 45°$ and $\theta_2 = 45° + \theta$.

If the second slot in a unit radiator is placed on the same radial line leaving the required $\lambda_0/4$ spacing between them, they will overlap. The second slot is shifted slightly in ϕ-direction to a different current-flow line (OB in Fig. 4) to avoid overlapping, and placed at the required distance ρ_2 from the origin. The position of the second slot in the pair has been calculated using the following approximate equations to a reasonable degree of accuracy:

$$\theta = \tan^{-1} \frac{\frac{\lambda_0}{4\sqrt{2}}}{\rho_1 + \frac{\lambda_0}{4\sqrt{2}}} \tag{8}$$

$$\rho_2 = \frac{\frac{\lambda_0}{4\sqrt{2}}}{\sin(\theta)} \tag{9}$$

C. SLOT ARRAY DESIGN

The next step is to appropriately fill the top plate with unit radiators. These unit radiators are arranged along a spiral, as shown in Fig. 5 so that the fields radiated by all unit radiators add constructively in the antenna boresight direction [3]. The spacing between two adjacent unit radiators in the radial direction (S_ρ in Fig. 5) is one of the design parameters. The spacing between two adjacent unit radiators along the spiral denoted by S_ϕ is another design parameter.

In this design, the widths and depths of all the slots were kept constant while their lengths were increased gradually with the radial distance away from the centre. Because the field strength inside the waveguide decreases from the centre towards the edge, the lengths of the slots need to increase gradually to make illumination more uniform over the aperture. The direction of the spiral ring on the plate determines whether the radiated circularly-polarized field is left-hand or right-hand. As the TEM mode is not fully established in the centre where the feed is, an area with a radius of P_{min} in the centre is left devoid of slots. As the two orthogonal slots in a unit radiator are spaced $\lambda_0/4$ apart, weak reflections from the two slots in the waveguide are out of phase and cancel each other.

III. EFFECTS OF PHYSICAL PARAMETERS

To investigate radiation characteristics, we have done a few parametric analyses, which are discussed below.

A. ANALYSIS I

The key to the low-cost dielectric-free and slow-wave free design is the reduction of the spacing between adjacent unit radiators in the radial direction from traditional $\lambda_\circ$ to a lesser value in order to avoid grating lobes. However, a large reduction would make radiation from adjacent unit radiators significantly incoherent, leading to a reduction in directivity and gain. Hence in this section, we have investigated radiation patterns when the spacing is reduced to $0.95\lambda_0$. For comparison and simulation simplicity, instead of actual unit radiators, for this initial analysis, we use dipole arrays with Hertzian dipoles replacing all unit radiators.

For this purpose, two dipole arrays were investigated with two different radial spacings, λ_0 (15 mm) and $0.95\lambda_0$ (14.2 mm), keeping other design parameters constant. The two corresponding arrays had 3224 and 3060 dipoles, respectively, in the locations of radiating slots of the corresponding RLSA and each dipole is directly excited with the correct phase. Both arrays have 14 rings of radiator pairs making a spiral geometry, as shown in Fig. 6. Fig. 7 and Fig. 8 show the computed radiation patterns of the dipole arrays at $\phi = 0°$ and $\phi = 90°$ plane, respectively, at 20 GHz. As it can be seen, $1\lambda_0$ radial spacing provides a directivity

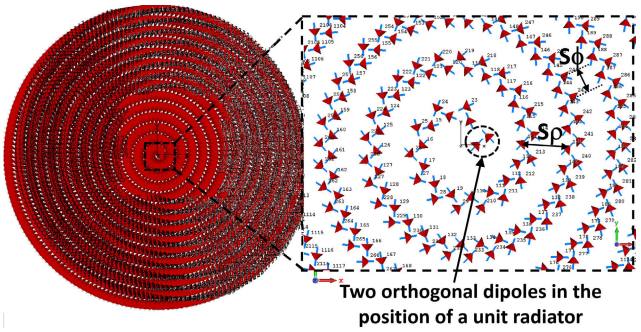

FIGURE 6. Dipoles arranged spirally, in a pattern similar to the radiating slots of the RLSA, replacing all the slots of the RLSA.

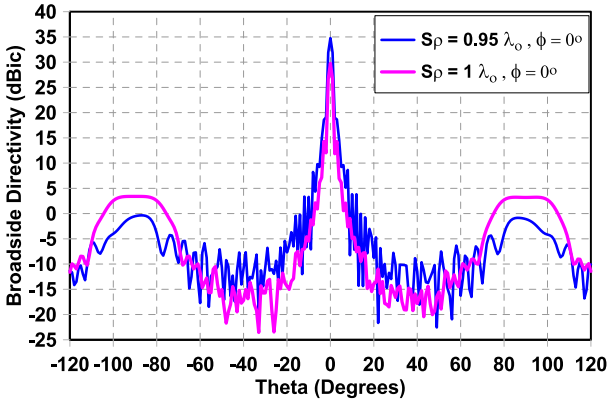

FIGURE 7. Radiation patterns of the dipole arrays on $\phi = 0°$ plane at 20 GHz.

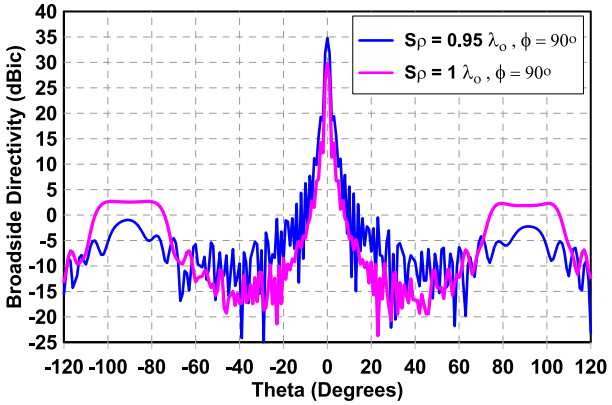

FIGURE 8. Radiation patterns of the dipole arrays on $\phi = 90°$ plane at 20 GHz.

of 29.7 dBic at 20 GHz, which is 5.8 dBic lower than the directivity (35.5 dBic) achieved with $0.95\lambda_0$ radial spacing. The dipole array with $0.95\lambda_0$ spacing also makes the highly significant lobe from $\theta = 70°$ to $110°$ weaker by about 5 dB, compared to $1\lambda_0$ spacing.

B. ANALYSIS II

In the second investigation, an RLSA was designed where radial separation S_ρ was kept constant at the design frequency while the angular separation S_ϕ is varied to change the density of unit radiators on the aperture of the RLSA. For the sake of comparison (with later design), dimensions of slots (slot length and width) were also kept constant. Lower S_ϕ effectively increases slot density and radiated power density. For this investigation, a physical aperture that is 27 λ_0 in diameter having 14 spiral turns of radiating slots were used. The value of S_ϕ was varied between $\lambda_0/3$ (5 mm) to λ_0 (15 mm) in steps of 1 mm. It is to mention here that S_ϕ cannot be reduced below a particular value of $\lambda_0/3$ to ensure that the unit radiators do not overlap. For each value of S_ϕ, the peak directivity and gain in the broadside direction, axial ratio and total efficiency within the operating frequency band are listed in Table 2.

TABLE 2. Antenna performance for different values of S_ϕ at 20 GHz.

S_ϕ	S_ρ	L	S_{11}	Directivity	Gain	Axial ratio	Efficiency
mm	mm	mm	dB	dBic	dBic	dB	%
5	14.2	5	-11.9	28.5	28.1	2.2	90
6	14.2	5	-11.4	27.4	27	2.2	90
7	14.2	5	-11.1	26.5	26.1	2.3	89
8	14.2	5	-10.8	25.8	25.3	2.3	89
9	14.2	5	-10.6	25.1	24.6	2.4	89
10	14.2	5	-10.6	24.4	23.9	2.4	89
11	14.2	5	-10.6	23.8	23.3	2.5	89
12	14.2	5	-10.6	23.3	22.8	2.6	89
13	14.2	5	-10.7	23	22.5	2.6	89
14	14.2	5	-10.7	22.8	22.3	2.6	89
15	14.2	5	-10	21.8	21.4	2.6	89

From Table 2 it can be seen that the antenna aperture with the lowest value of S_ϕ has the highest directivity, gain and total efficiency. As S_ϕ increases, the peak gain drops and the impedance matching slowly deteriorates.

C. ANALYSIS III

The coupling of energy from the travelling wave into the radiated wave through radiating slots is the most critical aspect that controls aperture illumination and hence radiation pattern of the antenna. The radial outward travelling wave within the RLSA waveguide generates surface currents on the top plate and thus excites radiating slots. The amount of energy that is coupled by the radiating slots depends on several parameters, including the total number of slots and slot density in the top plate. If all the unit radiators are arrayed on the CP-RLSA aperture with equal lengths and widths, then each slot couples almost a constant proportion of the radial current. As the power is fed at the centre of the CP-RLSA, more energy will radiate from the centre, and less energy will radiate from the edges. This will diminish the power intensity of the wave travelling outward within the waveguide by a factor of $\frac{1}{\sqrt{\rho}}$ through the coupling of the radiating slots, which is not favourable in terms of boresight gain. Hence a proper slot coupling analysis is necessary to control illumination over the CP-RLSA antenna aperture. One possible method is to keep the slot density constant ($S_\rho \times S_\phi =$ constant) on the

aperture and control the energy coupled by the unit radiators from the inner waveguide field to the radiating field.

In this investigation, the density of slot ($S_\rho \times S_\phi$) on the aperture was kept constant while the slots' lengths were varied to investigate the effect of various energy coupling from travelling wave into the space wave. For an RLSA with fixed slot density, the two parameters that control energy coupling are slot length (L) and slot inclination angles (θ_1, θ_2) to the current flow line. Since the slot inclination angles were fixed in this case, the slot length was varied on the antenna aperture. The slot length (L) of this RLSA can be represented as

$$L = \delta + (\rho \times \alpha) \tag{10}$$

where δ is a constant, ρ is the radial distance, and α is the coupling coefficient. The product ($\rho \times \alpha$) is the coupling factor and controls how much energy is coupled from the waveguide field to the radiated field. For a particular distribution, the coupling coefficient α needs to optimize. As the radial distance (ρ) increases, it is necessary to increase the coupling factor, which requires increasing slot length. By varying the slot length, we can control the proportion of energy coupled from the inner field to the radiating field.

Fig. 9 shows antenna performances for varying the fixed δ component of the slot length (L) at 20 GHz. To reduce the taper in the aperture amplitude distribution, α was fixed at 0.008. S_ρ and S_ϕ were set at $0.95\lambda_0$ and $0.4\lambda_0$, respectively, and the total number of slot pairs for this design is 1530. From Fig. 9 it can be seen that δ with a value of 5.2 provides the maximum gain with an axial ratio below 3 dB.

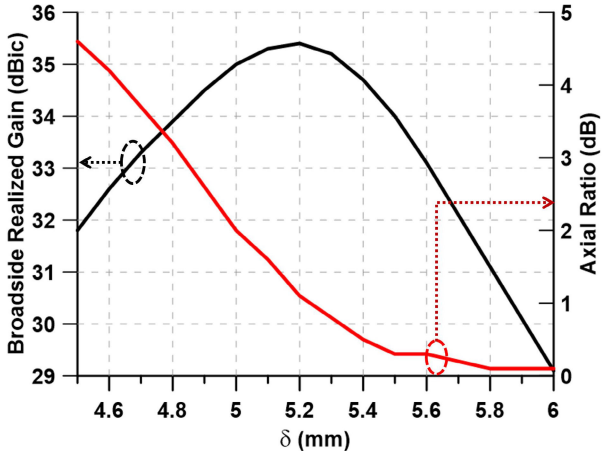

FIGURE 9. Variation of antenna performance with δ at 20 GHz. Note: slot length, $L = \delta + (\rho \times 0.008)$.

IV. RESULTS

To verify the design strategy, an antenna was designed, and the parameters of the final design are given in Table 3. The slot layout on the surface, shown in Fig. 5, was created using a custom made Visual Basic interface with CST Microwave Studio.

TABLE 3. Parameters of the fabricated antenna.

Main parameter	Symbol	Value (mm)
Free-space wavelength	λ_0	15
Slot length range	L	5.24 - 5.56
Slot width	W	1
Slot depth	D	0.5
Number of rings	N	14
Air waveguide height	d	5
Initial radius	ρ_{min}	5
Slot pair spacing in angular direction	S_ϕ	6
Slot pair spacing between two spiral rings	S_ρ	14.2
Aperture diameter	$27\lambda_0$	405

A. ANTENNA PROTOTYPE

The performance of the antenna was predicted by simulating it using the Transient Solver of CST Microwave Studio and both near-field, and far-field results were analyzed. The predicted results were later verified with measurements of a prototype. A picture of the prototype is shown in Fig. 10. The slot pattern on the top plate was made using laser cutting slots in a 0.5 mm thick sheet of stainless steel. Laser cutting was used because it was less expensive for prototyping compared to some other techniques such as water jet cutting. The drawback of laser cutting was the slotted plate was deformed at a few places due to intense heat dissipated by the laser beam when etching a fairly large number of slots in the metal sheet. To reduce the effects of deformation, a thicker bottom plate was used as the ground plane of the antenna, and the top plate was fixed above the thick bottom plate using twenty four-equally spaced 5 mm nylon spacers along the periphery of the two plates.

B. INPUT REFLECTION COEFFICIENT

The feeding probe was realized using a standard SMA connector glued to a customized disk head. The impedance matching of the antenna was verified using PNA-X vector network analyzer. Measured and predicted $|S_{11}|$ of the antenna, compared in Fig. 11, is well matched within the operating band from 19 GHz to 21 GHz. The difference in $|S_{11}|$ between the predicted and measured results can be attributed to the non-uniform waveguide height caused by the deformation of the top plate and accuracy of laser cutting used in manufacturing. The measured antenna has a very wide 10-dB return loss bandwidth of 45.4% from 16.7 GHz to 26.5 GHz. This is because of the $\lambda_0/4$ inter-element spacing between two orthogonal slots in a unit radiator of the CP-RLSA antenna. The reflected waves from successive slots arriving back at the input port are out of phase and cancel each other. Since all the slot pairs are arranged spirally, the total sum of reflections is almost zero at the antenna feed point. Therefore, the antenna demonstrates excellent matching over the frequency band of interest.

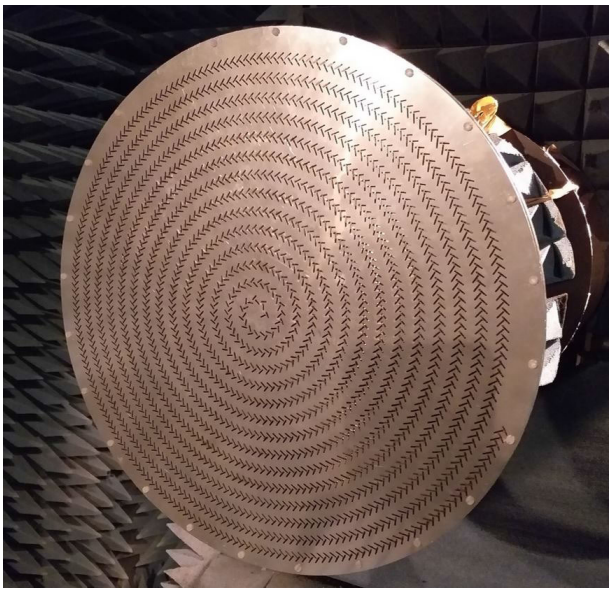

(a)

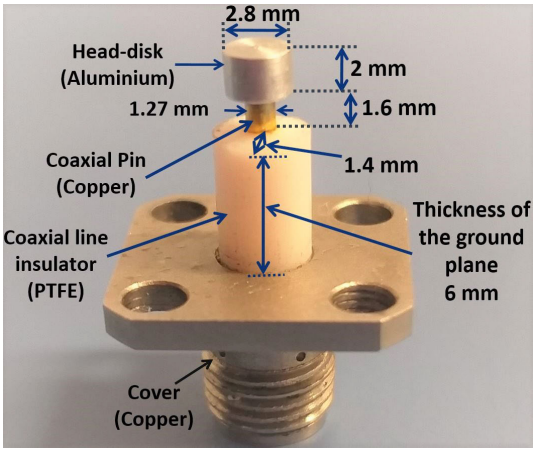

(b)

FIGURE 10. (a) Fabricated prototype, (b) Modified SMA connector with the disk-head.

C. DIRECTIVITY, GAIN AND EFFICIENCY

The peak directivity and gain of the antenna both in the broadside direction are shown in Fig. 12. The predicted antenna has a peak directivity of 36.8 dBic with a peak gain of 36.6 dBic at 20 GHz. The variation of peak gain and directivity with frequency is almost identical. The predicted 3-dB directivity bandwidth and 3-dB gain bandwidth are 6%, from 19.3 GHz to 20.5 GHz. The anechoic range did not allow accurate gain measurements beyond 20 GHz, and hence measured results are shown only up to that frequency. The antenna has a measured peak directivity of 36.3 dBic and a measured peak gain of 35.9 dBic at 19.7 GHz. The aperture efficiency of the antenna is 56%, and the total antenna efficiency is 95.4% at 19.7 GHz. Its radiation efficiency is excellent and varies between 96.9% and 97.4% in the operating frequency band, but gain measurement had to be limited to 20 GHz due to range limitations.

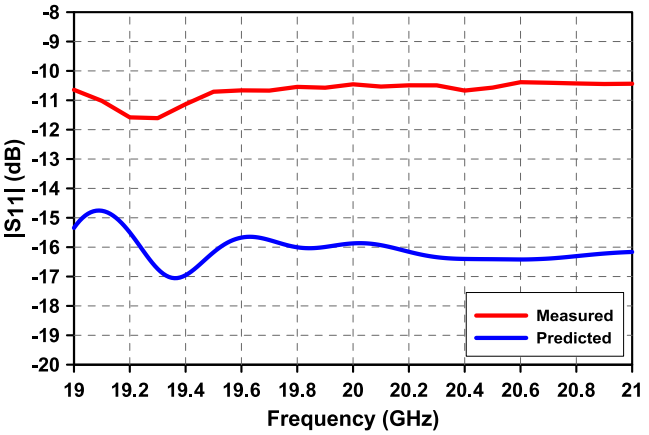

FIGURE 11. Reflection coefficient magnitude $|S_{11}|$ of the antenna prototype.

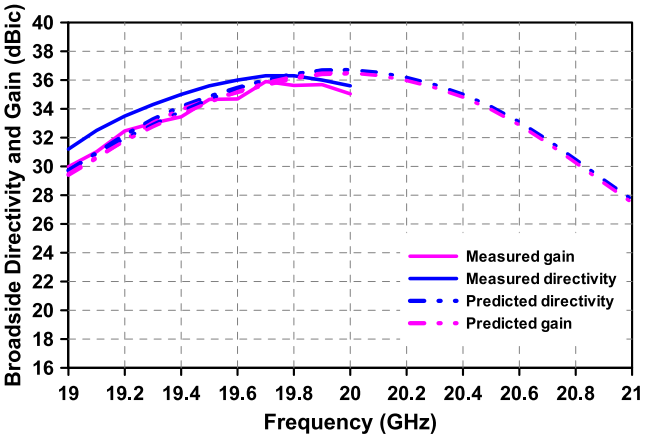

FIGURE 12. Broadside directivity and gain.

D. FAR-FIELD RADIATION

Fig. 13 shows the predicted radiation patterns at 20 GHz. In this figure, the cross-polar level in $\phi = 0°$ plane is 12.3 dBi in the broadside direction, which is 24.5 dB lower than the co-polar level. The antenna has stable far-field radiation patterns in the operating frequency band. To demonstrate this, predicted and measured far-field elevation pattern cuts taken at two azimuth angels $\phi = 0°$ and $\phi = 90°$ at six frequencies within the 3-dB directivity bandwidth are shown in Figures 14 to 19.

The predicted and measured patterns agree reasonably well with no significant side or grating lobe, but a minor shoulder lobe was captured in both predicted and measured results around the main peak. The antenna has shown a shoulder lobe of -16.8 dB in $\phi = 0°$ plane and -21.8 dB in $\phi = 90°$ plane at the operating frequency of 20 GHz. The measured antenna has shown cross-polar level 24.36 dB lower than the co-polar level at 20 GHz. The 3-dB beamwidth is 2.1° in $\phi = 0°$ plane and 2.2° in $\phi = 90°$ plane. Further, the antenna patterns in the operating band comply with ETSI (European Telecommunications Standards Institute) Class-1 radiation pattern envelope (RPE). All pattern cuts in

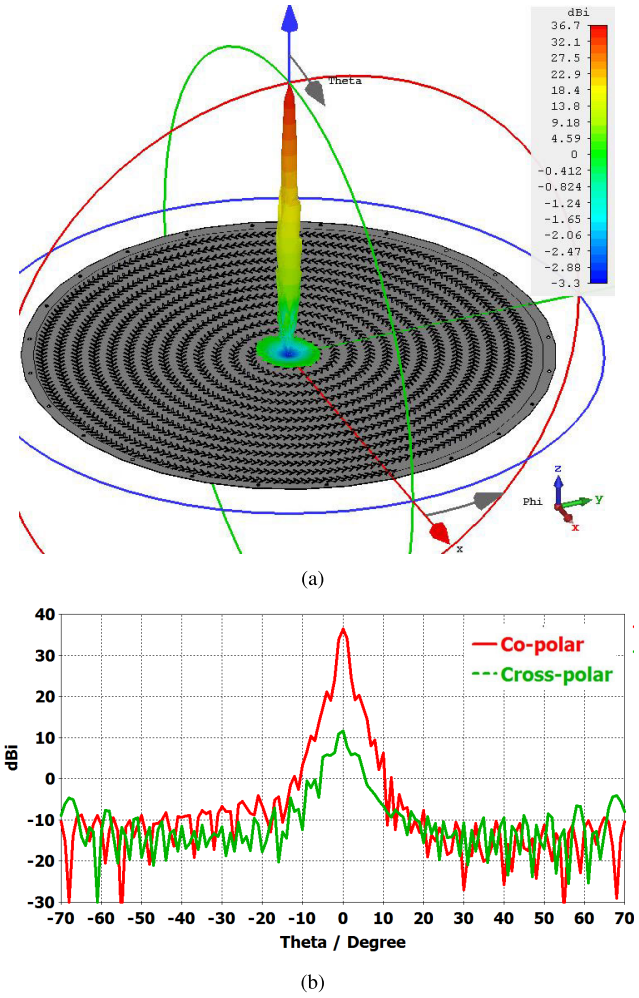

FIGURE 13. Predicted radiation pattern (a) 3D view of the far-field radiation pattern at 20 GHz, (b) 2D radiation pattern at $\phi = 0°$ plane at 20 GHz.

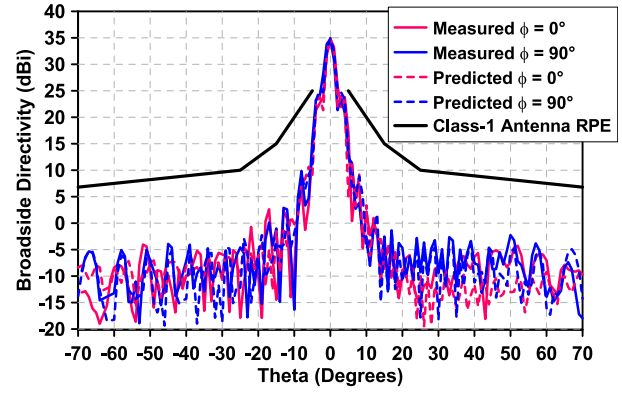

FIGURE 14. Far-field radiation patterns at 19.4 GHz.

$\phi = 0°$ and $\phi = 90°$ planes are compared with ETSI RPE in Figures 14 to 19.

E. AXIAL RATIO

The quality of circular polarization radiated by the antenna is quantified through broadside axial ratio shown in Fig. 20. The axial ratio predicted from simulation and obtained from

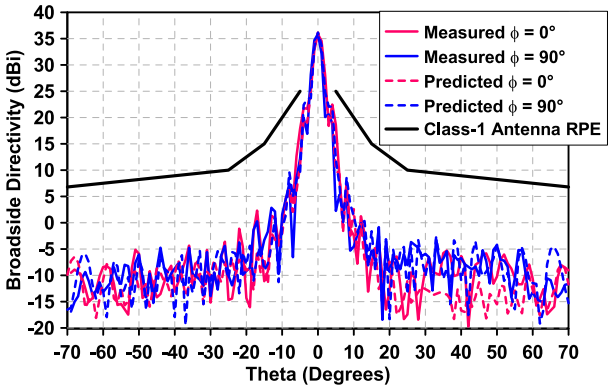

FIGURE 15. Far-field radiation patterns at 19.6 GHz.

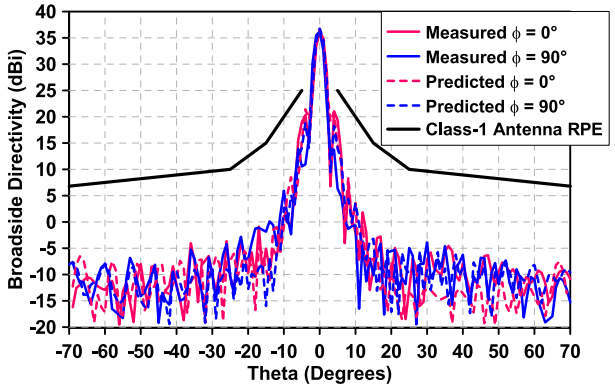

FIGURE 16. Far-field radiation patterns at 19.8 GHz.

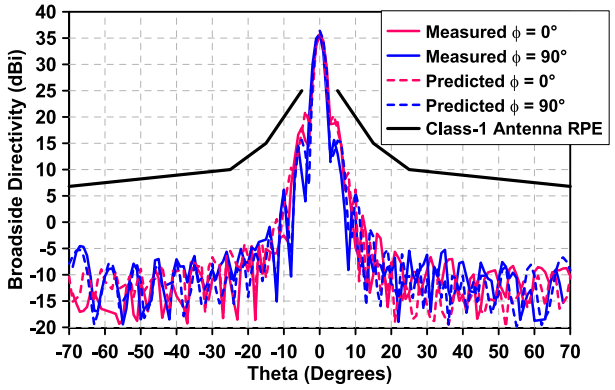

FIGURE 17. Far-field radiation patterns at 20 GHz.

measurements match closely and are lower than 3-dB over the operating frequency range. The predicted 3-dB axial ratio bandwidth of the antenna in boresight direction is 22.9% from 18.9 GHz to 23.8 GHz.

F. DISCUSSION

Table 4 summarizes the electrical and physical characteristics of the proposed all-metal single-layered CP-RLSA antenna comparing with some of the published conventional all-metal RLSA papers. Conventional all-metal double-layered RLSA antennas suffer from narrow radiation bandwidth, efficiency losses in the absorber and design complexity [26], [29], [30]. As it can be seen from the Table 4, our proposed RLSA

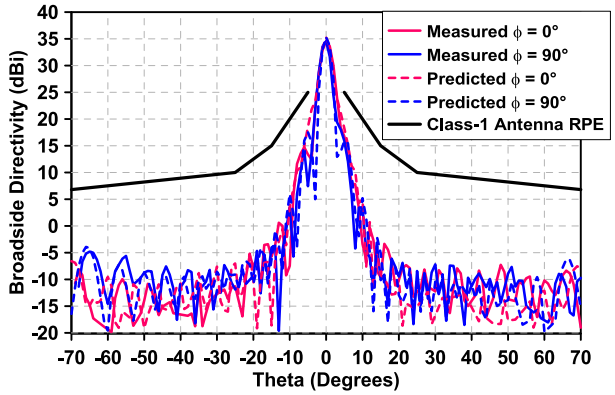

FIGURE 18. Far-field radiation patterns at 20.2 GHz.

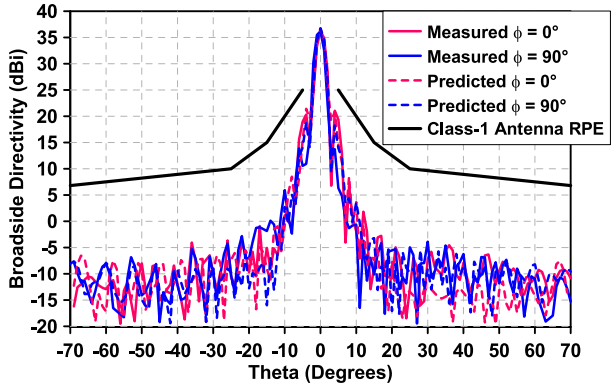

FIGURE 19. Far-field radiation patterns at 20.4 GHz.

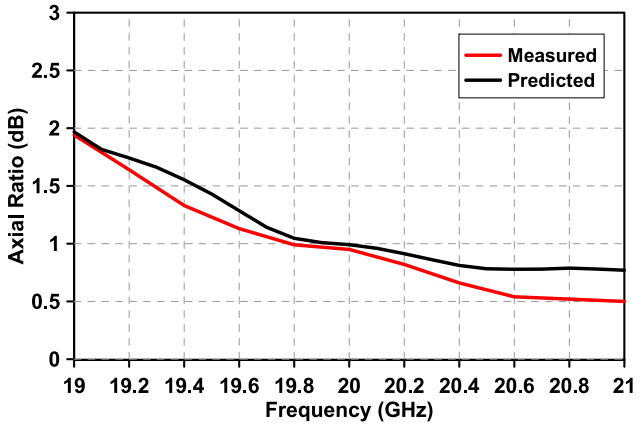

FIGURE 20. Axial ratio of the new antenna.

has shown a good aperture efficiency, a wider impedance bandwidth, higher total efficiency and lowest side lobe levels (SLL) compared to the previously reported all-metal RLSAs. The proposed RLSA does not require any dielectrics, slow-wave structure, absorber, reflection cancelling structure, phase tuning structure and mode converter, which greatly reduces the design complexity, cost and weight of the antenna. Due to the lack of absorber, the total antenna efficiency has increased. The losses of the proposed RLSA are very low and zero chances for radio frequency (RF) breakdown. Single-layered waveguide was used to design the proposed CP RLSA, which made the antenna compact and

TABLE 4. Comparison of the new all-metal CP-RLSA antenna with key previous works.

	This work	Ref. [26]	Ref. [29]	Ref. [30]	Ref. [9]
Waveguide	Single-layered	Double-layered	Double-layered	Double-layered	Single-layered
Directivity (dB)	36.3	31	32	31.5	33.5
Electrical height (λ_0)	0.43	4.7	3.2	3.1	0.5
Impedance bandwidth (%)	45.4	1	2.5	2.3	16
Total efficiency (%)	96.6	44.8	62.7	54	61
Aperture efficiency (%)	56	28	<55	55	61
SLL at operating frequency ($\phi = 90°$) (dB)	-21.8	-7	-11	-13.5	-17
Requires absorber	No	Yes	Yes	Yes	Yes
Requires slow-wave structure	No	Yes	Yes	Yes	No
Requires reflection cancelling structure	No	Yes	Yes	Yes	No
Requires phase tuning structure	No	Yes	Yes	Yes	No
Requires mode converter	No	No	Yes	No	Yes
Design and fabrication complexity	Simple	Highly Complex	Highly Complex	Complex	Complex
Cost	Low	High	High	High	Medium

robust. Compared to previously reported RLSAs, the electrical height of the new antenna is very low (less than $0.5\lambda_0$), provides the flexibility to be easily mounted on roof-top or wall which is suitable for satellite communication in moving platform.

V. CONCLUSION

We presented and demonstrated a design methodology for all-metal dielectric-less circularly polarized radial-line slot array (RLSA) antennas. An RLSA antenna made of a metal sheet with a slotted pattern is a low-cost solution for receiving satellite services and wireless backhauls. Experimental results prove the excellent performance of the antenna, which has a maximum measured gain of 35.9 dBic, aperture efficiency of 56% and low side lobe levels. The thickness of the antenna is only $0.43\lambda_0$ (6.5 mm) and it can be easily mounted on a roof-top of even a moving platform such as a long-distance bus or train. The antenna does not need any dielectric material whatsoever, so by replacing the insulator in the feed line with air, it can be made also useful for space systems where radiation hardness is required and high-power microwave systems where dielectrics can break down.

REFERENCES

[1] M. U. Afzal and K. P. Esselle, "Steering the beam of Medium-to-High gain antennas using near-field phase transformation," *IEEE Trans. Antennas Propag.*, vol. 65, no. 4, pp. 1680–1690, Apr. 2017.

[2] K. Kelly and F. Goebels, "Annular slot monopulse antenna arrays," *IEEE Trans. Antennas Propag.*, vol. 12, no. 4, pp. 391–403, Jul. 1964.

[3] M. Ando, K. Sakurai, N. Goto, K. Arimura, and Y. Ito, "A radial line slot antenna for 12 GHz satellite TV reception," *IEEE Trans. Antennas Propag.*, vol. 33, no. 12, pp. 1347–1353, Dec. 1985.

[4] M. Ando, K. Sakurai, and N. Goto, "Characteristics of a radial line slot antenna for 12 GHz band satellite TV reception," *IEEE Trans. Antennas Propag.*, vol. 34, no. 10, pp. 1269–1272, Oct. 1986.

[5] M. Ando, T. Numata, J.-I. Takada, and N. Goto, "A linearly polarized radial line slot antenna," *IEEE Trans. Antennas Propag.*, vol. 36, no. 12, pp. 1675–1680, Dec. 1988.

[6] M. Takahashi, J.-I. Takada, M. Ando, and N. Goto, "A slot design for uniform aperture field distribution in single-layered radial line slot antennas," *IEEE Trans. Antennas Propag.*, vol. 39, no. 7, pp. 954–959, Jul. 1991.

[7] J. Takada, M. Ando, and N. Goto, "A reflection cancelling slot set in a linearly polarized radial line slot antenna," *IEEE Trans. Antennas Propag.*, vol. 40, no. 4, pp. 433–438, Apr. 1992.

[8] M. Ando, "New DBS receiver antennas," in *Proc. 23rd Eur. Microw. Conf.*, Sep. 1993, pp. 84–92.

[9] K. Ichikawa, J.-I. Takada, M. Ando, and N. Goto, "A radial line slot antenna without a slow wave structure," *Electron. Commun. Jpn.*, vol. 76, no. 7, pp. 81–88, 1993.

[10] P. W. Davis and M. E. Bialkowski, "Experimental investigations into a linearly polarized radial slot antenna for DBS TV in australia," *IEEE Trans. Antennas Propag.*, vol. 45, no. 7, pp. 1123–1129, Jul. 1997.

[11] P. W. Davis and M. E. Bialkowski, "Linearly polarized radial-line slot-array antennas with improved return-loss performance," *IEEE Antennas Propag. Mag.*, vol. 41, no. 1, pp. 52–61, Feb. 1999.

[12] M. E. Bialkowski and P. W. Davis, "Analysis of a circular patch antenna radiating in a parallel-plate radial guide," *IEEE Trans. Antennas Propag.*, vol. 50, no. 2, pp. 180–187, Feb. 2002.

[13] N. Y. Koli, M. U. Afzal, K. P. Esselle, and M. Z. Islam, "Analyzing the coupling from radiating slots in a double-layered radial line slot array antenna," in *Proc. IEEE Int. Symp. Antennas Propag.*, Jul. 2019, pp. 1427–1428.

[14] S. I. Zakwoi, T. A. Rahman, I. Maina, and O. Elijah, "Design of ka band downlink radial line slot array antenna for direct broadcast satellite services," in *Proc. IEEE Asia–Pacific Conf. Appl. Electromagn. (APACE)*, Dec. 2014, pp. 159–162.

[15] A. Mazzinghi, M. Albani, and A. Freni, "Double-spiral linearly polarized RLSA," *IEEE Trans. Antennas Propag.*, vol. 62, no. 9, pp. 4900–4903, Sep. 2014.

[16] J. Suryana and D. B. Kusuma, "Design and implementation of RSLA antenna for mobile DBS application in ku-band downlink direction," in *Proc. Int. Conf. Electr. Eng. Informat. (ICEEI)*, Aug. 2015, pp. 341–345.

[17] M. Vera-Isasa, M. Sierra-Castaner, and M. S. Perez, "Design of circular polarized radial line slot antennas," *Int. J. Wireless Opt. Commun.*, vol. 1, pp. 179–189, Dec. 2003.

[18] N. Y. Koli, M. U. Afzal, K. P. Esselle, L. Matekovits, and Z. Islam, "Investigating small aperture radial line slot array antennas for medium gain communication links," in *Proc. Int. Conf. Electromagn. Adv. Appl. (ICEAA)*, Sep. 2019, pp. 0613–0616.

[19] M. Takahashi, M. Ando, N. Goto, Y. Numano, M. Suzuki, Y. Okazaki, and T. Yoshimoto, "Dual circularly polarized radial line slot antennas," *IEEE Trans. Antennas Propag.*, vol. 43, no. 8, pp. 874–876, Aug. 1995.

[20] M. Sierra-Castaner, M. Sierra-Perez, M. Vera-Isasa, and J. L. Fernandez-Jambrina, "Low-cost monopulse radial line slot antenna," *IEEE Trans. Antennas Propag.*, vol. 51, no. 2, pp. 256–263, Feb. 2003.

[21] T. Purnamirza, "Radial line slot array (RLSA) antennas," in *Telecommunication Systems*, A. A. Isiaka, P. P. Monteiro, and A. L. Teixeira, Eds. Rijeka, Croatia: IntechOpen, 2019, ch. 10.

[22] T. S. Lim and K. G. Tan, "The development of radial line slot array antenna for direct broadcast satellite reception," *Int. J. Electron.*, vol. 94, no. 3, pp. 251–261, Mar. 2007.

[23] M. Albani, A. Mazzinghi, and A. Freni, "Automatic design of CP-RLSA antennas," *IEEE Trans. Antennas Propag.*, vol. 60, no. 12, pp. 5538–5547, Dec. 2012.

[24] J. M. F. Gonzalez, P. Padilla, G. Exposito-Dominguez, and M. Sierra-Castaner, "Lightweight portable planar slot array antenna for satellite communications in X-band," *IEEE Antennas Wireless Propag. Lett.*, vol. 10, pp. 1409–1412, 2011.

[25] N. Y. Koli, M. U. Afzal, K. P. Esselle, and M. Z. Islam, "Comparison between fully and partially filled dielectric materials on the waveguide of circularly polarised radial line slot array antennas," in *Proc. Int. Workshop Antenna Technol. (iWAT)*, Feb. 2020, pp. 1–3.

[26] C.-W. Yuan, S.-R. Peng, T. Shu, Z.-Q. Li, and H. Wang, "Designs and experiments of a novel radial line slot antenna for high-power microwave application," *IEEE Trans. Antennas Propag.*, vol. 61, no. 10, pp. 4940–4946, Oct. 2013.

[27] I. Maina, T. A. Rahman, and M. Khalily, "Bandwidth enhanced and sidelobes level reduced radial line slot array antenna at 28 GHz for 5G next generation mobile communication," *ARPN J. Eng. Appl. Sci.*, vol. 10, pp. 5752–5757, 2015.

[28] R. A. A. Kamaruddin, I. M. Ibrahim, M. A. A. Rahim, Z. Zakaria, N. A. Shairi, and T. A. Rahman, "Radial line slot array (RLSA) antenna design at 28 GHz using air gap cavity structure," *J. Telecommun., Electron. Comput. Eng.*, vol. 9, nos. 2–8, pp. 133–136, 2017.

[29] S. Peng, C.-W. Yuan, T. Shu, J. Ju, and Q. Zhang, "Design of a concentric array radial line slot antenna for high-power microwave application," *IEEE Trans. Plasma Sci.*, vol. 43, no. 10, pp. 3527–3529, Oct. 2015.

[30] S. Peng, C. Yuan, T. Shu, and X. Zhao, "Linearly polarised radial line slot antenna for high-power microwave application," *IET Microw., Antennas Propag.*, vol. 11, no. 5, pp. 680–684, Apr. 2017.

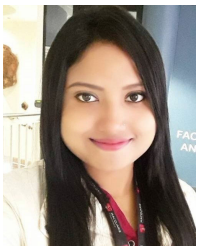

MST NISHAT YASMIN KOLI (Graduate Student Member, IEEE) received the B.S. degree in electronics and telecommunication engineering from the Rajshahi University of Engineering and Technology (RUET), Rajshahi, Bangladesh, in 2015, and the Master by Research (M.Res.) degree in electronics engineering from Macquarie University, Sydney, Australia, in 2017. She is currently pursuing the Ph.D. degree with the Centre for Collaboration in Electromagnetic and Antenna Engineering (CELANE), Macquarie University, Sydney, NSW, Australia.

From 2015 to 2016, she was a Lecturer with the Electrical and Electronics Engineering Department, European University, Dhaka, Bangladesh. Her research interests include antenna array, high-gain planar metasurface-based antennas, radial-line slot array antennas, beam steering metasurfaces, antennas for radio astronomy and satellite communication, and microwave and millimetre-wave antennas. She received several prestigious awards, including the prestigious "Macquarie University Medal", and the International Research Training Program Scholarship (iRTP) for the MRes and International Macquarie University Research Excellence Scholarship (iMQRES) for the Ph.D. degree.

MUHAMMAD U. AFZAL (Member, IEEE) received the B.S. degree (Hons.) in electronics engineering and the master's degree in computational science and engineering from the National University of Sciences and Technology (NUST), Islamabad, Pakistan, in 2005 and 2011, respectively, and the Ph.D. degree in electronics engineering from Macquarie University, in 2016.

From 2010 to 2012, he was a Lab Engineer with the Samar Mubarakmand Research Institute of Microwave and Millimeterwave Studies (SMRIMMS), Islamabad, Pakistan. From 2012 to 2013, he was a Lecturer with the Electrical Engineering Department, NUST, Islamabad, Pakistan. He is currently a Research Associate with the School of Electrical and Data Engineering, University of Technology Sydney. His research interests include electromagnetic band gap or Fabry-Perot resonator antennas, high-gain planar metasurface-based antennas, radial-line slot antennas, phased arrays, free-standing phase-shifting structures or metasurfaces, frequency selective surfaces, near-field phase transformation, and far-field pattern synthesis using near-field phase transformation.

Dr. Muhammad received NUST merit base scholarship during undergraduate studies and International Macquarie Research Excellence Scholarship (iMQRES) for Ph.D. studies.

KARU P. ESSELLE (Fellow, IEEE) received the B.Sc. degree (Hons.) in electronic and telecommunication engineering from the University of Moratuwa, Sri Lanka, and the M.ASc. and Ph.D. degrees with near-perfect GPA in electrical engineering from the University of Ottawa, Canada.

He was the Director of the WiMed Research Centre and the Associate Dean—Higher Degree Research (HDR) of the Division of Information and Communication Sciences and directed the Centre for Collaboration in Electromagnetic and Antenna Engineering, Macquarie University. He is currently the Distinguished Professor in electromagnetic and antenna engineering with the University of Technology Sydney and also a Visiting Professor of Macquarie University, Sydney. According to a Special Report on Research published by The Australian national newspaper in 2019, he is the National Research Field Leader in Australia in microelectronics in Engineering Discipline and in the Electromagnetism field in the Disciplines of Physics and Mathematics. He has authored approximately 600 research publications and his articles have been cited more than 9,700 times. In each of 2019 and 2018, his publications received more than 1,100 citations. He is the first Australian antenna researcher ever to reach Google Scholar h-index of 30 and his citation indices have been among the top Australian antenna researchers for a long time (at present: i10 is 174 and H-index is 48). Since 2002, his research team has been involved with research grants, contracts and Ph.D. scholarships worth about 20 million dollars, including 15 Australian Research Council grants, without counting the 245 million-dollar SmartSat Corporative Research Centre, which started in 2019. His research activities are posted in the web at and He has provided expert assistance to more than a dozen companies including Intel, the Hewlett Packard Laboratory, USA; Cisco Systems, USA; Audacy, USA; Cochlear, Optus, ResMed and Katherine-Werke, Germany. His team designed the high-gain antenna system for the world's first entirely Ka-band CubeSat made by Audacy, USA and launched to space by SpaceX, in December 2018. This is believed to be the first Australian-designed high-gain antenna system launched to space, since CSIRO-designed antennas in Australia's own FedSat launched in 2002. His research has been supported by many national and international organizations including Australian Research Council, Intel, U.S. Air Force, Cisco Systems, Hewlett-Packard, the Australian Department of Defence, Australian Department of Industry, and German and Indian governments.

Dr. Esselle served as a member for the Dean's Advisory Council and the Division Executive and as the Head for the Department several times. He is a Fellow of the Royal Society of New South Wales and Engineers Australia. His awards include the 2004 Innovation Award for best invention disclosure, the 2009 Vice Chancellor's Award for Excellence in Higher Degree Research Supervision, the 2011 Outstanding Branch Counsellor Award from IEEE headquarters (USA), the 2016 and 2012 Engineering Excellence Awards for Best Published Paper from IESL NSW Chapter, the 2017 Excellence in Research Award from the Faculty of Science and Engineering, the 2017 Engineering Excellence Award for Best Innovation, the 2017 Highly Commended Research Excellence Award from Macquarie University, the 2017 Certificate of Recognition from IEEE Region 10, the 2019 Motohisa Kanda Award (from IEEE USA) for the most cited article in the IEEE TRANSACTIONS on EMC in the past five years, the 2019 Macquarie University Research Excellence Award for Innovative Technologies, and the 2019 ARC Discovery International Award. His mentees have been awarded many fellowships, awards and prizes for their research achievements. Fifty international experts who examined the theses of his Ph.D. graduates ranked them in the top 5% or 10%. He is a Track Chair of the IEEE AP-S 2020 Montreal, a Technical Program Committee Co-Chair of ISAP 2015, APMC 2011, and TENCON 2013, and the Publicity Chair of ICEAA/IEEE APWC 2016, IWAT 2014, and APMC 2000. Since 2018, he has been chairing the prestigious Distinguished Lecturer Program Committee of the IEEE Antennas and Propagation (AP) Society – the premier global learned society dedicated for antennas and propagation - which has close to 10 000 members worldwide. After two stages in the selection process, he was also selected by this Society as one of two candidates in the ballot for 2019 President of the Society. Only three people from Asia or Pacific apparently have received this honor in the 68-year history of this Society. He is also one of the three Distinguished Lecturers (DL) selected by the Society in 2016. He is the only Australian to chair the AP DL Program ever, the only Australian AP DL in almost two decades, and second Australian AP DL ever (after UTS Distinguished Visiting Professor Trevor Bird). He has been continuously serving the IEEE AP Society Administrative Committee in several elected or ex-officio positions since 2015. He is also the Chair of the Board of management of Australian Antenna Measurement Facility. He was the elected Chair of both IEEE New South Wales (NSW), and IEEE NSW AP/MTT Chapter, in 2016 and 2017. He is an Associate Editor of the IEEE TRANSACTIONS ON ANTENNAS PROPAGATION and IEEE ACCESS. He is in the College of Expert Reviewers of the European Science Foundation, from 2019 to 2022. He has been invited to serve as an international expert/research grant assessor by several other research funding bodies as well, including the European Research Council and funding agencies in Norway, Belgium, The Netherlands, Canada, Finland, Hong Kong, Georgia, South Africa, and Chile. He has been invited by Vice-Chancellors of Australian and overseas universities to assess applications for promotion to professorial levels. He has also been invited to assess grant applications submitted to Australia's most prestigious schemes such as Australian Federation Fellowships and Australian Laureate Fellowships. In addition to the large number of invited conference speeches he has given, he has been an invited plenary/extended/keynote speaker of several IEEE and other conferences and workshops including EuCAP 2020 Copenhagen, Denmark; URSI'19 Seville, Spain; and 23rd ICECOM 2019, Dubrovnik, Croatia.

RAHEEL M. HASHMI (Member, IEEE) received the B.S. degree (Hons.) from CIIT, Pakistan, the M.S. degree from the Politecnico di Milano, Italy, and the Ph.D. degree from Macquarie University, Australia. From 2012 to 2015, he was a Visiting Researcher with the CSIRO Astronomy and Space Science Division, Australia. He is currently a Senior Lecturer with the Faculty of Science and Engineering, Macquarie University. He has contributed more than 80 peer-reviewed journals and conference papers, two scholarly book chapters. He is an inventor on two patent applications.His research interests include novel antenna technologies and microwave/millimeter-wave devices for applications in communications sector, defence, and smart living. His research explores the electromagnetic response of artificially engineered materials, using them to manipulate electromagnetic radiation for creating simple, yet highly efficient antennas and wireless components. He has received about two million dollars worth of research grants, contracts, and fellowships.

Dr. Hashmi was a recipient of several prestigious awards and fellowships, including the 2017 Young Scientist Award (Field and Waves) from the International Union of Radio Science (URSI), the 2012 Commonwealth IPRS Award, the CSIRO OCE Ph.D. Fellowship, and the Institute's Gold Medal from the CIIT, Pakistan. He was the Chair of the IEEE Antennas and Propagation/Microwave Theory and Techniques Joint Chapter from 2018 to 2019 and the Vice Chair of the IEEE Young Professionals Affinity Group in New South Wales from 2017 to 2018. He serves as an Associate Editor for the *IET Microwaves, Antennas and Propagation*, and as a Guest Editor for IEEE ACCESS, and *Microwave and Optical Technology Letters* (Wiley). He regularly reviews for several esteemed journals and conferences in his field, including the IEEE TRANSACTIONS ON ANTENNAS AND PROPAGATION, the IEEE ANTENNAS AND WIRELESS PROPAGATION LETTERS, IEEE ACCESS, the Asia–Pacific Microwave Conference, International Conference on Electromagnetics in Advanced Applications, AP-S Symposium, and EuCAP.